

## Supplementary Information

### Non-humidified proton conduction between a Lewis acid–base pair

*Takaya Ogawa, Hidenori Ohashi, Takanori Tamaki and Takeo Yamaguchi\**

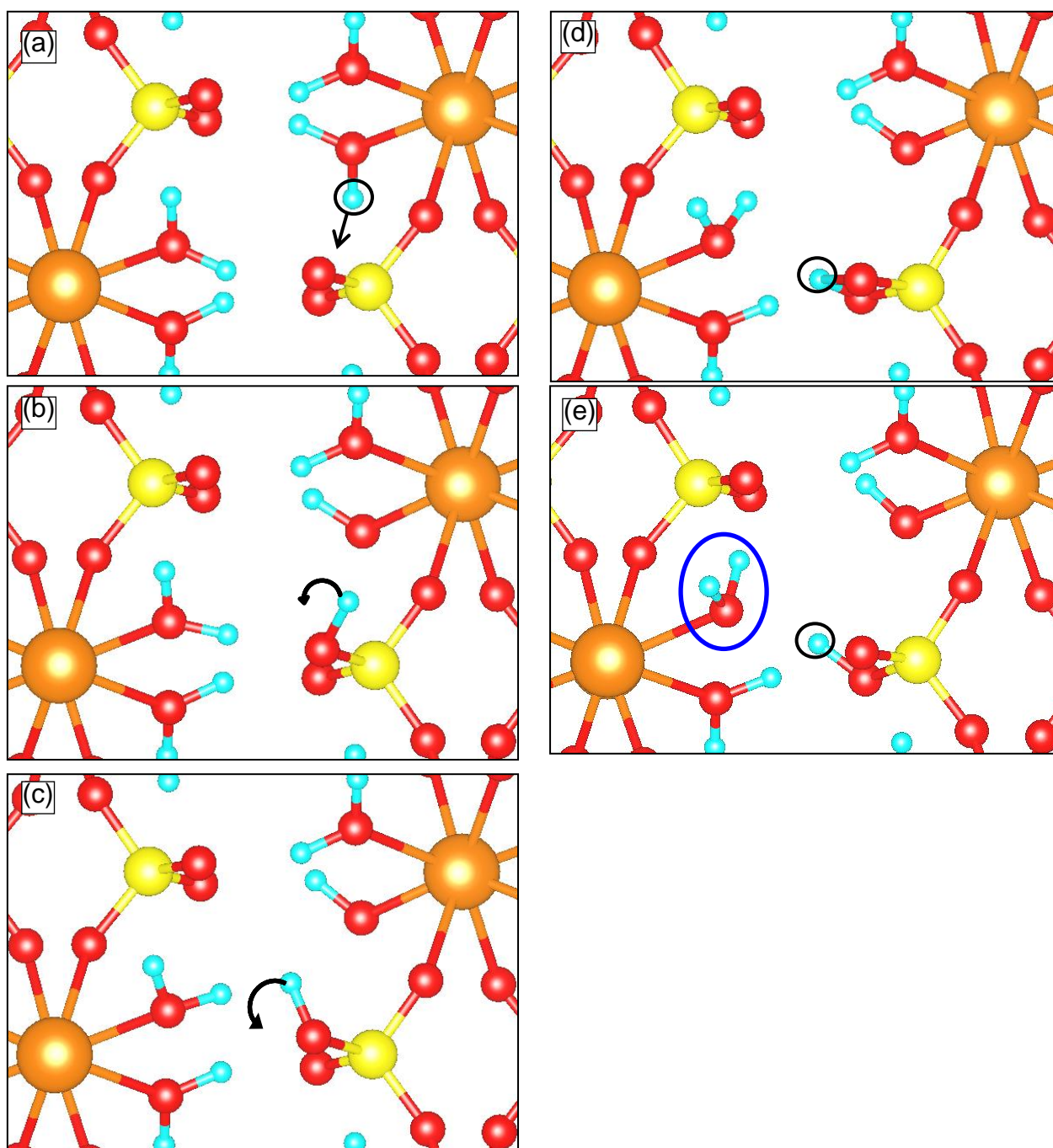
Chemical Resources Laboratory, Tokyo Institute of Technology, R1-17, 4259 Nagatsuta, Midori-ku, Yokohama 226-8503, Japan.

#### Proton conduction paths

We calculated 23 proton conduction paths in  $\text{ZrSO}_4$  besides the proton transfer path described in the main text. All proton conduction paths include plane or vertical transfer as an initial step. A typical proton conduction path is described as follows.

#### *Proton transfer from Lewis base to Lewis base*

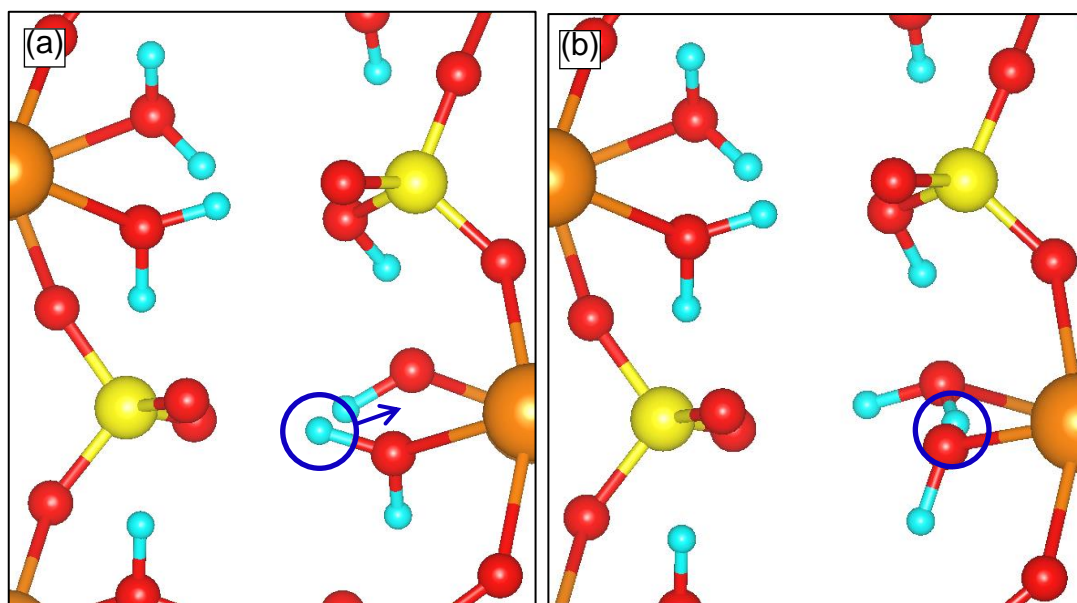
This proton transfer is one of the possible patterns after plane transfer. Figure S1(a) shows the initial structure of  $\text{ZrSO}_4$ . A proton moves to a Lewis base by plane transfer (Fig. S1(b)). The proton then reorients from the oxygen where it is initially positioned to another oxygen in  $\text{SO}_2$  (Fig. S1(c) and (d)). Finally, the proton stays at a different oxygen to the one that the proton was initially bonded to (Fig. S1(e)). The transition state of this process is given as Fig. S1(d) with a very high  $E_a$ , 290 kJ/mol. Since the transition state is 'the structure with the transferring proton stays between oxygen atoms in the same Lewis base', proton transfer from Lewis base to Lewis base takes place with difficulty at 90 °C. However, there exists feasibility of some sort of reorganizations that may occur, such as the reorientation of the blue-circled  $\text{H}_2\text{O}$  (depicted as Fig. S1(e)) to facilitate the transfer from Lewis base to Lewis base. The possible other proton transfer is suggested in the following sections.



**Supplementary Figure S1.** Proton conduction path to another oxygen in SO<sub>2</sub> via S=O in-plane transfer,  $E_a = 290$  kJ/mol. The colour scheme used is as follows: Zr, orange; S, yellow; O, red; H, blue (this applies to all figures). (a) The initial structure of ZrSO<sub>4</sub>. (b) A proton moves to a Lewis base by plane transfer. (c), (d) The proton then reorients from the oxygen, where it is initially positioned, to another oxygen in SO<sub>2</sub>. (e) Finally, the proton stays at a different oxygen to the one that the proton was initially bound to. There exists feasibility of some sort of reorganizations that may occur, such as the reorientation of the blue-circled H<sub>2</sub>O (in Fig. S1(e)) to facilitate the transfer from Lewis base to Lewis base

*Proton transfer from the next water bound to Lewis acid to OH<sup>-</sup>, water bound to Lewis acid in the absence of proton*

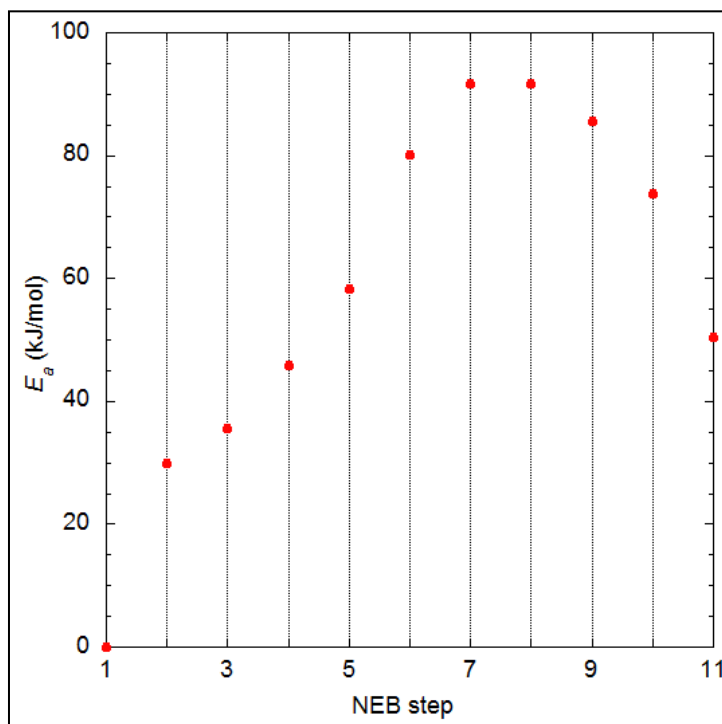
This proton transfer is also one of the possible patterns after plane transfer. The proton transfer from the adjacent water bound to Lewis acid to OH<sup>-</sup>, water bound to Lewis acid in the absence of proton, which is generated by the plane transfer, can happen with low  $E_a$ , 12.3 kJ/mol (Fig. S2). This newly obtained OH<sup>-</sup> can accept another proton from Lewis base, generated by another plane transfer. The  $E_a$  of proton transfer from Lewis base to OH<sup>-</sup> bound to Lewis acid is shown in the next section.



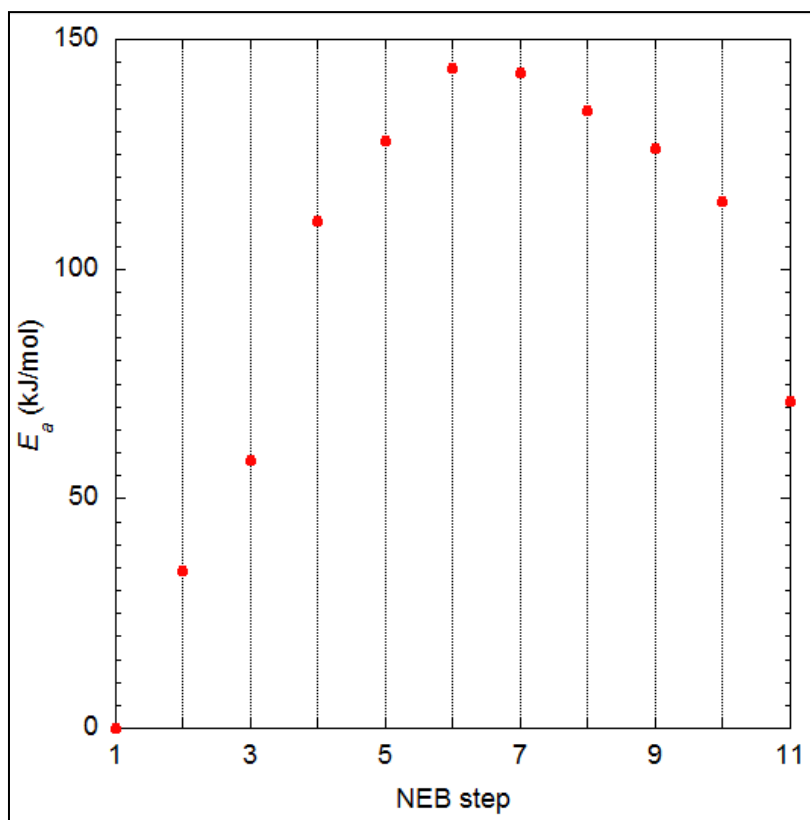
**Supplementary Figure S2.** Proton transfer from the adjacent water bound to Lewis acid to OH<sup>-</sup>, water bound to Lewis acid in the absence of proton. (a) The blue circled proton reorientates to the OH<sup>-</sup>, and (b) hop to the OH<sup>-</sup>.

*Proton transfer from Lewis base to OH bound to Lewis acid*

The energy values of each image during proton transfer, calculated by nudged elastic band (NEB) with 11 images, including the initial and final structures, are shown in Fig. S3 and S4. We can understand that plane and vertical transfer are single steps in terms of energy value. The average energy differences between the initial and final structures in plane transfer and vertical transfer are 48 and 82 kJ/mol, respectively; these result from proton transfer from Lewis acid to Lewis base. As mentioned in the main text, the average  $E_a$  values of plane transfer and vertical transfer are 88 and 142 kJ/mol, respectively. Hence, the average  $E_a$  values of reverse proton transfer from Lewis base to Lewis acid in the absence of a proton, in plane transfer and vertical transfer, are 40 and 60 kJ/mol, respectively. We can therefore conclude that proton transfer from Lewis base to Lewis acid in the absence of a proton is easier than proton transfers from Lewis acid to Lewis base. The combination of the proton transfer depicted in this section (Fig. S3), Fig. S2 and plane transfer are involved in a successive proton path.



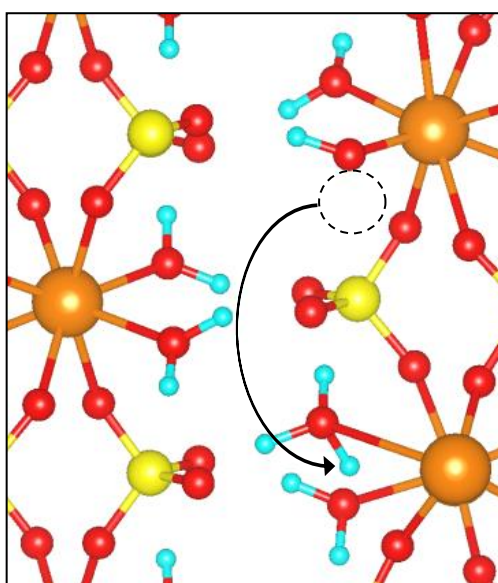
**Supplementary Figure S3.** An example of the energy values at each image of the plane transfer in the NEB calculation.



**Supplementary Figure S4.** An example of the energy values at each image of vertical transfer in NEB calculation.

### Determining the $\text{ZrSO}_4$ structure including $\text{H}_3\text{O}^+$

The  $\text{ZrSO}_4$  structure including  $\text{H}_3\text{O}^+$ , composed of the bound water and a proton from water bound to the Lewis acid, was determined. The proton from bound water was taken and allocated to the next to another bound water (Fig. S4). This structure was optimized without fixing the positions of the atoms. The average energy difference between the structure with  $\text{H}_3\text{O}^+$  and the initial structure is 106 kJ/mol. This value is higher than the energy difference between after and before plane transfer, 48 kJ/mol (Fig. S3). Therefore, proton is more stable in Lewis base than in water bound to Lewis acid as a  $\text{H}_3\text{O}^+$ .



**Supplementary Figure S5.** The structure including  $\text{H}_3\text{O}^+$ .

### Calculation method

The calculation method is described here. The density functional theory (DFT) calculations were performed using Revised Perdew–Burke–Ernzerhof (RPBE) functionals.<sup>S1</sup> Single Kleinman–Bylander projectors were used to represent each angular momentum channel,<sup>S2</sup> and a relativistic polarized calculation was used to estimate the effect of spin. A double- $\zeta$  split-valence basis set with polarization orbitals (DZP) was used.<sup>S3</sup> Norm-conserving pseudopotentials were applied using the improved Troullier–Martins method with non-linear core corrections.<sup>S4, S5</sup> These can accurately describe a hydrogen bond, essential for proton transfer. All of the calculations were performed with the Spanish Initiative for Electronic Simulations with Thousands of Atoms (SIESTA) 2.0.1 program.<sup>S4</sup> We applied the nudged elastic band (NEB) method to determine the transition state of proton transfer.<sup>S7-9</sup> VESTA software was used to visualize the crystal structures of  $\text{ZrSO}_4$ . Partial atomic electrostatic charges were computed with the Mulliken scheme.<sup>S10-12</sup> To calculate the

Mulliken charge of each atom, the basis set of hydrogen, DZP, was changed to the double- $\zeta$  split-valence basis set (DZ) while fixing the structure calculated with the DZP basis set for the reason given in Ref. 13. In the case of a single water molecule, the DZP basis set for the hydrogen atom including p-type orbitals gave the electron population number of the p-type orbital of the hydrogen atom as 0.178; the Mulliken atomic charge of protons then becomes a strange value,  $-0.052$ . By contrast, the Mulliken charge of protons with DZ for hydrogen and DZP for oxygen atoms while fixing the optimized geometry with the DZP basis set is  $+0.23$  in the case of a single water molecule, which is a reasonable value. Therefore, in this paper, we determined the optimized and transition state structures using the DZP basis set for all atoms and then calculated the Mulliken charge using the DZ basis set for hydrogen and the DZP basis set for all other atoms. It should be noted that the above observation on the Mulliken atomic charge of protons calculated with too many polarization orbitals is also a feature of the quantum chemistry calculation with the LCAO approximation.<sup>S13</sup>

### Calculation model

The  $\text{ZrSO}_4$  crystal structure was obtained from the experimental crystal data from the Inorganic Crystal Structure Database (ICSD). The size of a unit cell is  $26.8 \text{ \AA} \times 12.2 \text{ \AA} \times 5.8 \text{ \AA}$ , including four symmetrical layers and 32 water molecules, composed of 8 Zr atoms, 16 S atoms, 96 O atoms, and 64 H atoms. The space group of  $\text{ZrSO}_4$  is referred to as P1. The structure was optimized by the above calculation method using periodic boundary conditions with  $2 \times 2 \times 2$   $k$ -grid sampling. The proton transfer is described by the following steps. The optimized structure is the initial state (reactant). From reactant geometry, we moved one of the protons in the water bound to a Lewis acid and placed it near a sulphonyl base; we then optimized the geometry while fixing the positions of the moved proton and the proton-donating and/or -accepting oxygen atoms. Finally, all the atoms were optimized, and the final states (products) were obtained. To determine the transition states and minimum energy paths that connect the reactant and the product, we applied the NEB method. In determining the transition state, we eliminated two layers irrelevant to proton transfer to reduce calculation costs. The positions of atoms irrelevant to proton transfer remained fixed.

### Experimental method

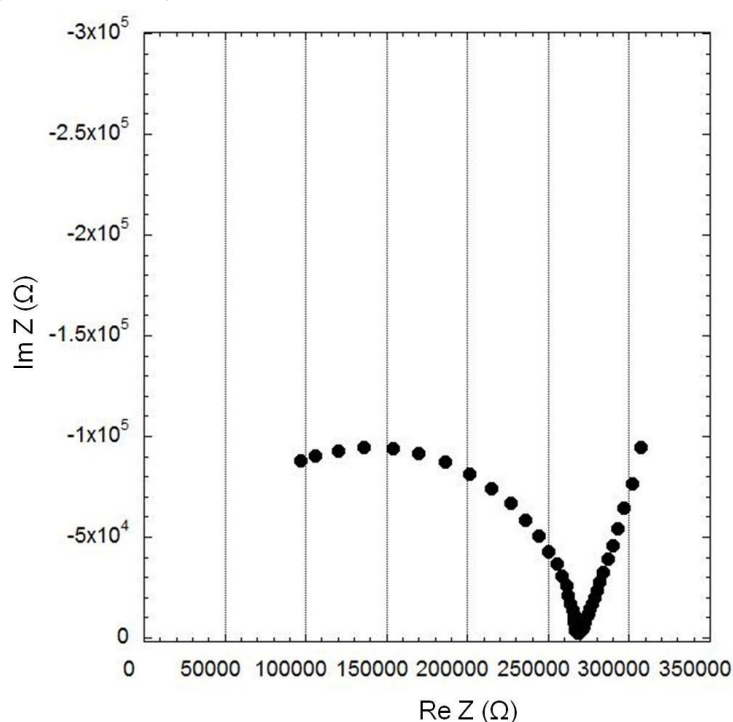
$\text{ZrSO}_4 \cdot 4\text{H}_2\text{O}$  (99.99% purity) was purchased from Wako Pure Chemical Industries, Ltd. (Osaka, Japan). A  $\text{ZrSO}_4$  pellet was made by pressing the  $\text{ZrSO}_4$  powder with 2 t for 5 min. The diameter of pellet was 13 mm. The density was  $0.366 \pm 0.006 \text{ g cm}^{-3}$ . Proton conductivity was measured using the two-probe AC impedance method with a Solartron 1260 Impedance/Gain Phase Analyzer in the frequency range of 1–10 MHz and at signal amplitude of 100 mV. The  $\text{ZrSO}_4$  pellet was set in a sample holder, SH2-Z, supplied by the Toyo Corporation, in which the electrode was changed to Pt.



The measurement conditions were controlled by a bench-top-type temperature (and humidity) chamber SH-221, supplied by ESPEC. Proton conductivity was obtained from the following equation:

$$\sigma = \frac{d}{R\pi r^2}$$

where  $R$ ,  $d$ , and  $r$  are the resistance, thickness of pellet, and radius of the electrode, respectively. A typical impedance plot is shown in Fig. S6. Resistance in this case is 33543  $\Omega$ , read from the fitting result using the points in the highest and lowest Im  $Z$  values of the left arc.



**Supplementary Figure S6.** A typical impedance plot

#### References

- S1 Hammer, B.; Hansen, L. B.; Nørskov, J. K. *Phys. Rev. B* 1999, **59**, 7413.
- S2 Kleinman, L.; Bylander, D. M. *Phys. Rev. Lett.* 1982, **48**, 1425.
- S3 Junquera, J.; Paz, O.; Sanchez-Portal, D.; Artacho, E. *Phys. Rev. B* 2001, **64**, 235111.
- S4 Troullier, N.; Martins, J. L. *Phys. Rev. B* 1991, **43**, 1993
- S5 Troullier, N.; Martins, J. L. *Phys. Rev. B* 1991, **43**, 8861
- S6 K. Momma, F. Izumi, *J. Appl. Crystallogr.*, 2008, **41**, 653
- S7 Gonzalez-Garcia, N.; Pu, J.; Gonzalez-Lafont, A.; Lluch, J. M.; Truhlar, D. G. *J. Chem. Theory Comput.* 2006, **2**, 895.
- S8 Henkelman, G.; Uberuaga, B. P.; Jonsson, H. *J. Chem. Phys.* 2000, **113**, 9901.
- S9 Ohto, T., Rungger, I., Yamashita, K., Nakamura, H., Sanvito, S., *Phys. Rev. B* 2013, **87**, 205439



- S10 Mulliken, R. S. J. Chem. Phys. 1955, **23**, 1833.
- S11 Csizmadia, I. G. J. Mol. Struct. 1976, **41**, 163.
- S12 Bickelhaupt, F. M.; van Eikema Hommes, N. J. R.; Fonseca, Guerra, C.; Baerends, E. J. Organometallics 1996, **15**, 2923.
- S13 Martin, F.; Zipse, H. J. Comput. Chem. 2005, **26**, 97.